Physica B 404 (2009) 370–372

Contents lists available at ScienceDirect

Physica B

journal homepage: www.elsevier.com/locate/physb

# Comparative study of organic metals and high-$T_c$ cuprates

S. Barišić [a,*], O.S. Barišić [b]

[a] Department of Physics, Faculty of Science, University of Zagreb, Bijenička c. 32, HR-10000 Zagreb, Croatia
[b] Jožef Stefan Institute, SI-1000 Ljubljana, Slovenia and Institute of Physics, Bijenička c. 46, HR-10000 Zagreb, Croatia

A B S T R A C T

The Bechgaard salts and the high $T_c$ cuprates are described by two and three band models, respectively, with the lowest band (nearly) half filled. In organics the interactions are small, while in cuprates the repulsion $U_d$ on the Cu-site is the largest energy. The Mott-AF state is stable in undoped materials in both cases. In the metallic phase of cuprates the $U_d \to \infty$ limit produces a moderate effective repulsion. The theories of the coherent SDW and charge-transfer correlations in the metallic phases of organics and cuprates are thus similar. In (undoped) organics those correlations are associated with commensurate $2k_F$ SDW and $4k_F$ bond or site modes. The corresponding modes in metallic cuprates are the incommensurate SDW and in particular $O_x/O_y$ quadrupolar charge transfer with wave vector $2q_{SDW} = q_0 + G$. They are enhanced for dopings $x > 0$, which bring the Fermi level close to the van Hove singularity. Strong coupling to the lattice associates the static incommensurate $O_x/O_y$ charge transfer with collinear "nematic" stripes. In contrast to organics, the coherent correlations in cuprates compete with local $d_{10} \leftrightarrow d_9$ quantum charge-transfer disorder.



## 1. Introduction

The high-$T_c$ cuprates are usually described by the Emery model [1] where the role similar to the external dimerization [2] in the Bechgaard salts is played by the Cu–O hopping $t_{pd}$, which puts two oxygens in the $CuO_2$ unit cell and makes the lowest of three bands half filled. The weak coupling theory at zero doping $x$ is then a quite straightforward analogue [3–6] of the 1D theory, provided that the imperfect nesting associated with the $O_x$–$O_y$ hopping $t_{pp}$ is ignored. The appearance of the $x = 0$ Mott-AF state is essentially independent of the value of $\Delta_{pd} = \varepsilon_p - \varepsilon_d > 0$ where $\varepsilon_d$ and $\varepsilon_p$ are the Cu and O site energies in the hole picture, respectively.

However, while the Hubbard repulsion in the Bechgaard salts is small, in the high-$T_c$ cuprates the repulsion $U_d$ on the copper site is the largest energy [1]. It has long been maintained [3,4] that the fundamental question in the high-$T_c$ cuprates concerns the nature of correlations which reduce $U_d$. The relevant $U_d = \infty$ limit is usually taken starting from the unperturbed state with average Cu-occupation $n_d^{(0)} = 1$. The lowest order process shown in Fig. 1a then corresponds to the fact that two holes on the neighboring Cu-sites can hop simultaneously to the intermediate O-site, empty at $x = 0$, provided that their spins are opposite. This leads to the superexchange [7] $J_{pd} \sim t_{pd}^4/\Delta_{pd}^3$ which is the basis of the $t$–$J$ models [7]. Alternatively, one can assume that all holes in the unperturbed metallic state are on the O-sites, i.e., that $n_d^{(0)} = 0$. When two p-holes of opposite spin are crossing the intermediate empty Cu-site one hole hops to the Cu-site when $t_{pd}$ is turned on, while the other has to wait as long as the Cu-site is occupied. The waiting time is of the order of $(\varepsilon_d - \mu)^{-1}$ where $\mu$ is the chemical potential of the two holes. The whole process of Fig. 1b consists of two independent $t_{pd}^2/(\varepsilon_d - \mu)$ hoppings, one per particle, and of the waiting time. Therefore the resulting effective $U_d = \infty$ repulsion $\tilde{U}$ of two p-particles is of the order of

$$\tilde{U} \sim t_{pd}^4/(\varepsilon_d - \mu)^3 \tag{1}$$

and can be interpreted as a retardation (kinematic) effect.

## 2. $U_d = \infty$ slave particle theory of the metallic phase

We have carried out the corresponding systematic theory which starts from the $n_d^{(0)} = 0$ unperturbed metallic ground state by using the slave particles. This time dependent diagrammatic approach, of infinite order in the perturbation $t_{pd}$, requires the use of the spinless fermion-Schwinger boson representation in order to avoid the degeneracy of the $n_d^{(0)} = 0$ unperturbed ground state in the overcomplete slave particle Hilbert space. The advantage of this representation is that the perturbation theory is manifestly translationally invariant at each stage, and ultimately locally gauge invariant. The disadvantage is that the three sorts of particles involved, $p^\sigma$-fermions, f-spinless fermions and Schwingers $b^\sigma$-bosons are distinguishable, i.e., that the Cu–O anticommutatiom rules are replaced by commutations. The theory has to be therefore antisymmetrized *a posteriori*. Here, we only quote the results.

* Corresponding author.
*E-mail address:* sbarisic@phy.hr (S. Barišić).

0921-4526/$ - see front matter © 2008 Elsevier B.V. All rights reserved.
doi:10.1016/j.physb.2008.11.025

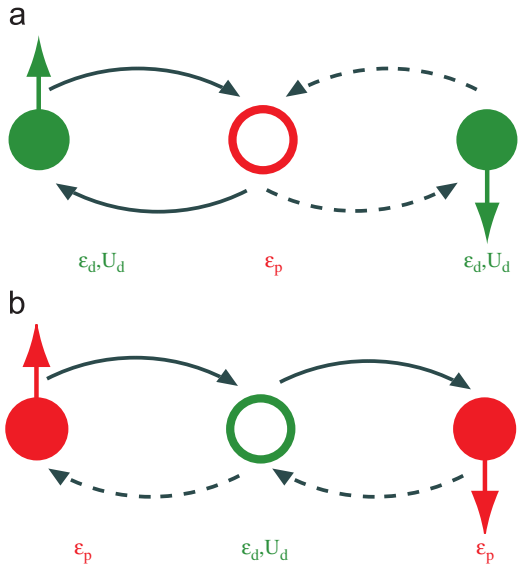


**Fig. 1.** (Color online) (a) Superexchange of two holes on Cu-sites via the empty oxygen site and (b) scattering of two holes on the O-sites via the empty Cu-site.

First, the omission of the Cu–O anticommutation rules is irrelevant in the lowest $r=1$ order of the Dyson perturbation theory. The reason is that the Cu site is initially empty, while one particle on Cu is required for anticommutation and two for $U_d$ interaction. This makes the $r=1$ expression for physical single-particle propagators strictly equivalent to the result of the $t_{pd}$ hybridized HF theory. The HF theory is expressed in terms of two hybridized propagators, one which starts and finishes with the appropriately weighted propagation on the O-sites (*pdp* propagator hereafter) and the other begins and ends on the Cu-sites (*dpd* propagator). Both propagators are characterized by the three $i=$ L, I, U bands of poles (branches) at $\omega_k^{(i)}$ [8]. This holds irrespectively of the average HF occupation $n_d^{(1)}$ of the Cu-site associated with the chemical potential $\mu^{(1)}$. On the other hand, the relations required ultimately by the local gauge invariance $n_f+n_b=1$ and $n_d=n_b$ are nearly satisfied at $r=1$ only when $n_d^{(1)}$ is small, i.e., the theory then converges quickly. It is therefore important to keep in mind that [3,6] $n_d^{(1)}\approx\frac{1}{2}$ at $|x|$ small for $t_{pd}\gg\Delta_{pd}$ and that finite $t_{pp}$ decreases it [8] further. The overall rule of thumb is that $n_d^{(1)}<\frac{1}{2}$ as long as the HF chemical potential $\mu^{(1)}$ falls below the vH singularity in the lowest L-band, i.e., as long as $x<x_{vH}$ where [8] $x_{vH}\propto -t_{pp}$ is the positive doping required to reach the vH singularity. As easily seen, small $n_d^{(1)}$ corresponds to a weak effective interaction $\tilde{U}<t_{pd}$.

The Cu–O (anti)commutation rules are also irrelevant for two further $r=2,3$ expressions. $r=2$ leads to the coherent Brinkman–Rice-like band narrowing $t_{pd}^2\to t_{pd}^2(1+n_d/2)(1-n_d)$ and the variation of $\Delta_{pd}$ through $\varepsilon_d\to\tilde{\varepsilon}_d$. However, unlike in the mean-field [8–10] slave particle approximations, this is accompanied by the incoherent, local, dynamic fluctuations identified as the $d_{10}\leftrightarrow d_9$ charge-transfer disorder. Importantly, the disorder falls far from the Fermi level, although there are indications [10–12] that in higher perturbation orders it spreads all over the spectrum.

The interaction $\tilde{U}$ appears explicitly for $r=4$. It introduces the particle–particle and particle–hole correlations in the single particle *pdp* and *dpd* propagations. $\tilde{U}>0$ favorizes the coherent particle–hole correlations which appear here as pseudogaps. The slave fermion theory predicts however that the effect of $\tilde{U}$ is the same in the singlet and the triplet channels, which is the consequence of the omission of the Cu–O anticommutation rules. The *a posteriori* antisymmetrization of the theory therefore associates $\tilde{U}$ with the singlet (SDW) scattering only.

The relevant SDW hole–electron correlations are associated to lowest order with the *pdp*−*pdp* bubble, as suggested by Fig. 1b, where $\tilde{U}$ appears as the effective interaction between p-particles. In contrast, the corresponding small $U_d$ theory [3,5,6] involves the *dpd*−*dpd* bubble. However, although the spectral densities of the *pdp* and *dpd* propagators are complementary, the poles are the same. The associated elementary intraband bubbles share therefore the properties of the overlap of the vH singularities and of the (imperfect) Fermi surface (FS) nesting, which both favor the coherent SDW fluctuations with a dominant $\vec{q}_{SDW}$.

As mentioned above, $\mu^{(1)}$ in the vicinity of the vH singularity brings the metallic $U_d=\infty$ theory into the intermediate $\tilde{U}\approx t_{pd}$ regime with $n_d^{(1)}\approx\frac{1}{2}$. Various experiments and NQR in particular [13] indicate indeed that for $|x|\leqslant 0.2$ the average occupation of the Cu-site is close to $n_d\approx\frac{1}{2}$. Therefore, we associate the transition, between the $|x|\approx 0$ long- and short-range magnetic order and the metallic phase at finite $|x|$, to the crossover in $x$ between the $|x|\approx 0$ $t$−$J$ regime and the finite $|x|$ metallic regime considered here. This latter is characterized by the close competition of the $d_{10}\leftrightarrow d_9$ charge-transfer disorder and the coherence effects which is difficult to cover analytically. In this light, we shall identify below the physical content of the important hole–electron correlation functions and determine when their coherent limit is consistent with experiments in the metallic phase.

## 3. Coherent e–h correlations and stripes

Let us start with the SDW correlations for $x\approx x_{vH}>0$. The vH overlap/FS nesting behavior of the elementary intraband particle–hole bubble is not universal. It is however well known that $Re\chi_{SDW}^{LL}(\vec{q},\omega)$ becomes large for $\omega$ small and close to $\pi/a$ [1, 1]. Taking formally $t_{pp}=0$, the log square singularity in $\omega$ occurs [5,3] at $x=0$ due to the vH overlap and to the perfect 2D FS nesting at $\vec{q}_{SDW}=\pi/a$ [1, 1]. Analytical [14] and numerical [15] calculations show that imperfect nesting associated with finite $x$ at $t_{pp}=0$ produces spikes at incommensurate $\vec{q}_{SDW}^{coll}$ along the zone main axes. With finite $t_{pp}$ the spikes were also obtained numerically [16] for $\vec{q}_{SDW}^{dg}$ along its diagonals. While it seems well established [17] that the spikes at $\vec{q}_{SDW}^{coll}$ are dominated by the pairing of holes and electrons close to the antinodal $\pi/a$ [1, 0] and $\pi/a$ [0, 1] vH points, the pairing which gives rise to the spikes at $\vec{q}_{SDW}^{dg}$ is not yet determined unambiguously.

The single well-defined collinear $\pm\vec{q}_{SDW}^{coll}$ leg or the nearly circular $|\vec{q}_{SDW}|$ is observed clearly by the magnetic neutron scattering [18–20]. As a rule, $\vec{q}_{SDW}^{coll}$ appears for small energy transfers while $|\vec{q}_{SDW}|$ occurs at high frequencies, e.g., in metallic YBCO [19]. The observation of the strong leading harmonics is consistent with metallic coherency in the propagation of $t_{pd}$-hybridized particles. There is however also good NMR evidence [21] that non-magnetic disorder is present in LSCO. It may well correspond, in part, to the local $d_{10}\leftrightarrow d_9$ charge disorder, which is dynamic in the present theory but becomes frozen [21,22] by the strong coupling [23] to the heavy lattice.

The Emery model also encompasses [23] the $Cu/O_2$ and $O_x/O_y$ charge transfers and various bond fluctuations within the unit cell. In the $\vec{q}\to 0$ limit the $D_4$ symmetry classifies [24–26] those correlations in $A_{1g}$, $B_{1g}$ and $B_{2g}$ irreducible representations, the bond fluctuations being involved directly [26] into the Raman responses. The elementary bubbles associated with those correlations differ through coherence factors in their numerators while their respective poles and integration ranges are the same [26]. The $\vec{q}=0$ $B_{1g,2g}$ modes are dominated [26], respectively, by the

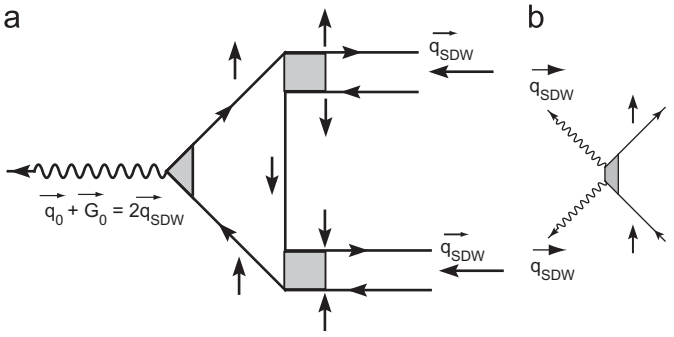


**Fig. 2.** Umklapp coupling of two SDWs enhanced at $\vec{q}_{SDW}$ (a) to intracell charge fluctuations and/or to phonons linearly coupled to carriers and (b) to phonons coupled quadratically to the carriers. Internal structure of the electronic triangle is governed by the $A_g$, $B_g$ symmetry properties of the outcoming vertices and by the $U_d$ or $\tilde{U}$ nature of the incoming square vertices which flip the spins.

contributions from the main axes or diagonals of the $CuO_2$ zone. They have their own small $\vec{q}$ structures [15,16] (e.g., the elementary $O_x/O_y$ bubble is logarithmically singular [3,23] at $x = x_{vH}$). In addition, while the $\vec{q} \approx 0$ $B_{1g}$ and $B_{2g}$ intracell modes are decoupled from the $\vec{q} \approx 0$ transfers of the total $CuO_2$ charge among the distant unit cells [15,23,26], the coherent $\vec{q} \approx 0$ $Cu/O_2$charge transfer is accompanied [15,26] by the $\vec{q} \approx 0$ intercell charge transfer. Only the latter is subject to the long-range Coulomb screening/frustration [15,22,26,27].

The small $\vec{q}$ behavior of the charge-transfer correlations is however of secondary interest if the SDW is taken [14] as the dominant fluctuation. Then, according to Fig. 2, two SDWs enhanced at $\vec{q}_{SDW} \approx \pi/a[1,1]$ either couple to the intracell fluctuations and then to phonons, or else directly to phonons. In the case of linear coupling of Fig. 2a the corresponding dominant $\vec{q}_0$ is small and satisfies the physically important relation

$$\vec{q}_0 + 2\pi/a\,[1,1] = 2\vec{q}_{SDW}. \tag{2}$$

Alternatively, as in Fig. 2b, two such SDWs can also couple quadratically [23] to tilts of the $CuO_6$ octahedra at $\vec{q}_{TILT} = \vec{q}_{SDW}$. When two SDWs enhanced at $\vec{q}^{\,coll}_{SDW}$ close to $\pi/a\,[1,1]$ are associated with the $\pi/a\,[1,0], \pi/a\,[0,1]$ pairing they drive [26], via the $B_{1g}$ $O_x/O_y$ charge transfer, the LTT/$(e_{xx}$-$e_{yy})$ deformations at $\pm\vec{q}^{\,coll}_{TILT}/\pm\vec{q}^{\,coll}_0$. Analogously, *if* two SDWs enhanced at $\vec{q}^{\,dg}_{SDW}$ close to $\pi/a\,[1,1]$ are associated with the $\pi/a\,[\frac{1}{2},\frac{1}{2}], \pi/a[-\frac{1}{2},-\frac{1}{2}]$ pairing they drive [26] the $B_{2g}$ $O_x$–$O_y$ bond fluctuations and the LTO/$(e_{xy}+e_{yx})$ modes at $\pm\vec{q}^{\,dg}_{TILT}/\pm\vec{q}^{\,dg}_0$.

The $\vec{q}_{TILT} \approx \pi/a\,[1,1]$ tilts and the $\vec{q}_0$ modes are in addition entangled [28] by the ionic forces, namely the $\pi/a\,[1,1]$ LTT and LTO tilts are accompanied, respectively, by the *homogeneous* $e_{xx} - e_{yy}$ and $e_{xy} + e_{yx}$ shears of the $CuO_2$ planes. Those entangled single leg deformations thus lift, through the electron–phonon couplings [23], the degeneracy of two $O_x/O_y$ sites [23] or of four $t_{pp}$ bonds within the $CuO_2$ unit cell by dimerizing them two by two.

The stability of the striped structures can be investigated using the related [14,23] Landau functionals. E.g., the entangled collinear modes are related in this way to the collinear nematic static stripes [27,29] usually characterized by $\vec{q}^{\,coll}_0$. It appears thus quite clearly that the coherent $O_x/O_y$ charge transfer, coupled to the lattice, is an essential ingredient of the collinear stripes [27] in the metallic phase. This agrees with observations [18,19,24,25,30,31]. The collinear SDW and $O_x/O_y$ charge-transfer correlations get enhanced in metallic lanthanum cuprates for dopings $x \approx x_{vH}$. The spikes [17] at $\vec{q}^{\,coll}_{SDW}$ in $\chi^{L,L}_{SDW}(\vec{q},\omega)$ then explain the "nematic" version of Eq. (2) observed [18,24] in the metallic phase. The corresponding LTO/LTT lattice instability is predicted [23] and observed [32,33] to be of the first order in LBCO for $x \approx x_{vH} \approx \frac{1}{8}$. Those effects are attributed here to the vH overlap/FS nesting, while the commensurability $\frac{1}{8}$ is expected to play only the secondary role.

In contrast to lanthanum cuprates the Fermi level $\mu$ in the optimally doped YBCO and BSCO, as measured by ARPES, falls [8] well below the vH point, i.e., $x < x^{HTC}_{vH}$. The collinear SDW-$O_x/O_y$ stripes enhanced by the vH singularities are therefore not expected to occur in metallic YBCO and BSCO. Indeed, at larger $x$, the collinear stripe structure is replaced [25] by the fourfold commensurate stripes in "checkerboard" configuration [25,34], which restores the $D_4$ symmetry.

The salient new feature of the present low-order large $U_d$ analysis is thus that the coherent, weak, incommensurate collinear [17] SDW and $O_x/O_y$ correlations appear to get enhanced with respect to the $d_{10} \leftrightarrow d_9$ charge disorder if the vH singularities are reached [35] by doping $x_{vH}$. This explains the long standing puzzle [32] why the enhanced magnetic/charge coherence occurs twice in LBCO as a function of doping, once as the long- or short-range [4,36] AF order at $x \approx 0$ and then again as the incommensurate SDW at single $\pm\vec{q}^{\,coll}_{SDW}$ for finite positive $x_{vH} \approx 0.1$, accompanied by the static $O_x/O_y$ charge transfer coupled to the staggered LTT tilting of the $CuO_4$ octahedra.

## Acknowledgments

Invaluable discussions with J. Friedel, L.P. Gor'kov, I. Kupčić, D.K. Sunko and E. Tutiš are gratefully acknowledged. This work was supported by the Croatian Government under Project nos. 119-1191458-0512 and 035-0000000-3187.

## References

[1] V.J. Emery, Phys. Rev. Lett. 58 (1987) 2794.
[2] S. Barišić, S. Brazovskii, in: J.T. Devreese (Ed.), Recent Developments in Condensed Matter Physics, vol. 1, Plenum, New York, 1981, p. 327.
[3] J. Friedel, J. Phys. Cond. Matt. 1 (1989) 7757.
[4] J. Friedel, M. Kohamoto, European Phys. J. B 30 (2002) 427.
[5] I.E. Dzyaloshinshii, V.M. Yakovenko, ZhETF 94 (1988) 344.
[6] S. Barišić, I. Batistić, Phys. Scripta T 27 (1989) 78.
[7] F.C. Zhang, T.M. Rice, Phys. Rev. B 37 (1987) 3759.
[8] I. Mrkonjić, S. Barišić, European Phys. J. B 34 (2003) 69.
[9] G. Kotliar, P.A. Lee, N. Read, Physica C 153–155 (1989) 538.
[10] L. Janković, D.K. Sunko, Physica C 341–348 (2000) 2103.
[11] H. Nikšić, E. Tutiš, S. Barišić, Physica C 241 (1995) 247.
[12] M.B. Zölfl, Th. Maier, Th. Pruchke, J. Keller, European Phys. B 13 (2000) 47.
[13] I. Kupčić, S. Barišić, E. Tutiš, Phys. Rev. B 57 (1998) 8590.
[14] H.J. Schulz, Phys. Rev. Lett. 64 (1990) 1445.
[15] E. Tutiš, H. Nikšić, S. Barišić, in: Lecture Notes in Physics, vol. 427, Springer, Berlin, 1997, p. 1.
[16] J.-H. Xu, T.J. Watson-Yang, J. Yu, A.J. Freeman, Phys. Lett. A 120 (1987) 489.
[17] Q. Si, Y. Zha, K. Levin, Phys. Rev. B 47 (1993) 9055.
[18] J.M. Tranquada, et al., Nature 429 (2004) 534.
[19] C. Stock, et al., Phys. Rev. B 71 (2006) 024522.
[20] V. Hinkov, et al., Science 319 (2008) 597.
[21] L.P. Gor'kov, G.B. Teitel'baum, J. Phys.: Conf. Ser. 108 (2008). 12009.
[22] L.P. Gor'kov, A.V. Sokol, JETP Lett. 46 (1987) 420.
[23] S. Barišić, J. Zelenko, Sol. St. Comm. 74 (1990) 367.
[24] A.G. Gozar, et al., in: Frontiers in Magnetic Materials, vol. 755, Springer, Berlin, 2005.
[25] L. Tassini, W. Prestel, A. Erb, M. Lambacher, R. Hackl, Phys. Rev. B 78 (2008) 020511(R).
[26] I. Kupčić, S. Barišić, Phys. Rev. B 75 (2007) 094508.
[27] S.A. Kivelson, et al., Rev. Modern Phys. 75 (2003) 1201.
[28] B. Piveteau, C. Nougera, Fizika 21 (1989) 237.
[29] V.J. Emery, S.A. Kivelson, Physica C 209 (1993) 597.
[30] A. Bianconi, et al., Phys. Rev. Lett. 76 (1996) 3412.
[31] S. Sugita, T. Watanabe, A. Matsuda, Phys. Rev. B 62 (2000) 8715.
[32] J.D. Axe, et al., Phys. Rev. Lett. 62 (1989) 2751.
[33] H. Kimura, et al., J. Phys. Soc. Japan 74 (2005) 445.
[34] T. Hanaguri, et al., Nature 430 (2004) 1001.
[35] A. Ino, et al., Phys. Rev. B 65 (2002) 094504.
[36] J. Lorenzana, G.A. Sawatzky, Phys. Rev. B 52 (1995) 9576.